

# ADDITIVE MANUFACTURE OF ROCKET ENGINE COMBUSTION CHAMBERS USING THE ABD<sup>®</sup>-900AM NICKEL SUPERALLOY

VIRTUAL CONFERENCE / 17 - 19 MARCH 2021

Iain Waugh<sup>(1,3)</sup>, Ed Moore<sup>(1)</sup>, Adam Greig<sup>(1)</sup>, James Macfarlane<sup>(1)</sup>, and William Dick-Cleland<sup>(2)</sup>

<sup>(1)</sup> Airborne Engineering Ltd., Westcott Venture Park, Aylesbury, HP18 0XB, UK

<sup>(2)</sup> Alloyed, 15 Oxford Industrial Park, Oxford, OX5 1QU, UK

<sup>(3)</sup> Corresponding author: iain@ael.co.uk

## KEYWORDS:

Additive manufacture, combustion chamber, IN718, ABD<sup>®</sup>-900AM

## ABSTRACT:

Nickel superalloys are a common material for liquid rocket engine combustion chambers, due to their high mechanical strength at high temperatures. The new ABD<sup>®</sup> series of alloys have been designed specifically for additive processes, with the ABD<sup>®</sup>-900AM alloy able to maintain strength up to 900°C, demonstrating an increase in temperature capability over IN718 of ~100°C. This paper describes the potential for use of ABD<sup>®</sup> alloys for combustion chamber manufacture in order to increase performance, and demonstrates the first firing of an ABD<sup>®</sup>-900AM combustion chamber.

## 1. INTRODUCTION

Liquid rocket engine combustion chambers require materials that can withstand the high thermal stresses at the firewall, which are governed by the heat flux, thermal conductivity, wall thickness, compliance and mechanical properties at elevated temperature. Typical material options for high performance rocket engines are either copper, nickel or aluminium alloys. Copper alloys have a high thermal conductivity and therefore a relatively low firewall temperature for a given heat flux, but they lose mechanical strength at a relatively low temperature. Nickel alloys have a much lower thermal conductivity, and therefore a high firewall temperature for a given heat flux, but are able to maintain mechanical strength at high temperatures.

Nickel alloys also have a lower susceptibility to sulphur accelerated corrosion than copper at high temperature [1], which is important for increasing chamber lifetime when using impure hydrocarbons as coolant.

Additive manufacture of rocket engine components has been demonstrated using several nickel alloys, most commonly with Inconel 625 (IN625) and 718 (IN718). They have been used with SLM for injectors [2, 3, 4], combustion chambers [3] and turbomachinery [5]. They have also been used with a variety of techniques for combustion chamber closeout, such as Laser Wire Direct Closeout [6], or for nozzle fabrication with the DED blown powder process [7].

Of the nickel superalloys originally designed for casting and forging processes, IN718 exhibits good suitability for additive manufacturing, whereas many stronger high-temperature alloys crack significantly during the process. It has been shown to be printable with higher values of yield strength, ultimate strength, elongation (A5) and reduction of area (Z) than cast or forged equivalents [2].

The ABD<sup>®</sup> series of nickel superalloys has recently been designed by Alloyed specifically for additive manufacturing, allowing the crack-free manufacture of higher-performance parts [8]. One of these, ABD<sup>®</sup>-900AM, maintains strength up to 900°C, demonstrating an increase in temperature capability over IN718 of ~100°C, whilst still being easily processable with similar parameters. A chamber made from ABD<sup>®</sup>-900AM therefore potentially allows for higher heat fluxes than IN718, with only very minor changes to the manufacturing process. This paper describes the construction and test firing of a demonstrator combustion chamber in ABD<sup>®</sup>-900AM, in a collaboration between Airborne Engineering (AEL), Alloyed and Renishaw.

## 2. ALLOYS-BY-DESIGN (ABD<sup>®</sup>)

The microstructural mechanisms that strengthen superalloys also make their processing challenging, due to the tendency of the material to crack. This is particularly apparent in the SLM process, because the thermally-induced residual stresses can be very high. Many existing nickel superalloys are thus unsuitable for additive manufacture. To fully exploit the design freedom of SLM, new alloys are required that are designed specifically for the process. Traditional methods for development of new alloys use slow and costly cycles of experimental iteration, which are not only inefficient but are also not guaranteed to find the optimal composition for an application. To address this, Alloyed's proprietary Alloys-by-Design (ABD<sup>®</sup>) software was developed to enable the rapid, cost-efficient development of new alloys that can be tailored to a specific application or manufacturing process, in this case high-temperature nickel alloys for SLM.

The ABD<sup>®</sup> software [9] uses a range of physics-based and machine learning models to predict the performance of millions of alloy compositions simultaneously, combining advancements in metallurgical understanding with computing horsepower to shorten the development cycle from years to a few weeks. From these millions of possible alloys, Alloyed's metallurgists work with engineers of the end application to determine the relevant performance metrics – in the case of complex SLM combustion chambers, high temperature strength and 'additive manufacturability' are key. Analysis tools are then used to perform trade-offs across all the performance metrics, reducing the number of viable compositions until one globally optimal alloy is identified for manufacture [8].

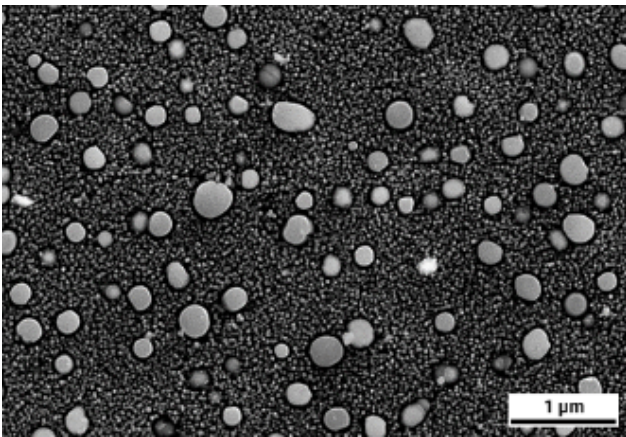


Figure 1: ABD<sup>®</sup>-900AM microstructure.

## 3. COMPARISON OF ABD<sup>®</sup> AND IN718

The highest performing ABD<sup>®</sup> alloy currently available for AM is ABD<sup>®</sup>-900AM, although it is still relatively new to the market. ABD<sup>®</sup>-900AM maintains strength up to 900°C, demonstrating an increase in temperature capability over IN718 of ~100°C. This extra temperature margin gives the potential for higher heat fluxes than IN718.

Nickel combustion chamber performance is typically limited by the high thermal gradients at the firewall. The potential gain in heat flux can be quantified by examining the stresses in the firewall, which consist of two main components: a pressure stress based on the pressure difference between the coolant and local chamber pressure value, and the thermal stress based on the thermal gradient in the firewall and the difference in thermal expansion of the cold and hot sides. A single coolant channel is modelled here, where the firewall is considered as a beam with fixed (not pinned) ends, due to the line of symmetry in between channels.

When a plate has a uniform pressure load and is fixed on two sides, then the maximum stress in that plate at the supports is [11]:

$$\sigma_{press} = -\frac{pw^2}{2t^2} \quad (1)$$

where  $w$  is the width between walls,  $t$  is the plate thickness and  $p$  is the pressure. Assuming the firewall is a flat plate with temperature difference across it and fixed ends, then the maximum compressive stress on the hot wall [11] is:

$$\sigma_{thermal} = \frac{\Delta T \alpha E}{2(1 - \nu)} \quad (2)$$

where  $\alpha$  is the coefficient of thermal expansion,  $E$  is the modulus of elasticity and  $\nu$  is the Poisson ratio.

In most rocket configurations the thermal stress will dominate at the throat, although the pressure stress may dominate in nozzle expansions where channels are wide and heat flux is low. Given that the throat stresses usually dominate in a chamber, the thermal stress is therefore considered as the limiting factor for the chamber design. For thermal stress alone, equation 2 can be rearranged to give the maximum heat flux for given values of yield stress ( $\sigma_y$ ), thermal conductivity ( $k$ ), modulus of elasticity and Poisson's ratio, where all of these are a function of temperature.

$$\dot{q}_{max} = \frac{k\Delta T}{t} = \frac{2k\sigma_y(1 - \nu)}{tE\alpha} \quad (3)$$

The maximum theoretical heat flux before reaching the yield stress can therefore be calculated from the previous expression if a coolant-side temperature is assumed; for hydrocarbon fuels this is usually a fair assumption because this is usually a limiting factor due to coking. The temperature limit for coking of typical fuels such as RP-1, methane and propane varies widely in the literature, because it is highly dependent on the fuel, the purity (particularly sulphur content), material and flow speed [12]. In general, the coking limits seems to be higher for nickel tubing rather than copper tubing where RP-1 or propane are used [12, 1] due to lower susceptibility to sulphur based corrosion.

Fig. 2 assumes a coolant side temperature of 650K, and plots the heat flux through the wall,  $k\Delta T/t$ , using temperature-averaged thermal conductivity (dashed lines), and also plots the maximum allowable heat flux for yield,  $(2k\sigma_y(1-\nu))/(tE\alpha)$ , based on maximum temperature properties (solid lines). The point where the dashed and solid lines meet defines the maximum heat flux for yield at the firewall, assuming no contribution from pressure stress. Values for the temperature variation of yield stress are taken from as-printed material results, as are the thermal conductivity and thermal expansion values for ABD<sup>®</sup>-900AM. Other values for  $E$  or  $\nu$  have been taken from non-additive literature sources and assumed to be the same for both ABD<sup>®</sup>-900AM and IN718 [13].

Fig. 2 demonstrates that the extra  $\sim 100^\circ\text{C}$  before strength drop-off translates to a  $\sim 14\%$  increase in maximum heat flux for ABD<sup>®</sup>-900AM over IN718. With the assumption that heat flux and chamber pressure are related by  $\dot{q}_{max} \propto p_c^{0.8}$ , this extra heat flux corresponds to a  $\sim 18\%$  increase in chamber pressure, which will result in an increase in specific impulse. This performance increase is dependent on the propellant combination and pressure, but for a typical LOX/RP-1 application might amount to  $\sim 2\%$ . In reality, the calculation above is a simplification and the quantitative value of maximum heat fluxes for a LOX/RP-1 engine will be higher than given in Fig. 2. This is because the analysis above does not include any carbon-deposit layer on the firewall or the result of any film-cooling or zoned-combustion, but the relative merit of the two materials should stand. Furthermore, ABD<sup>®</sup>-900AM should also be less prone to cracking and likely to have better surface roughness than IN718, and has significantly better creep performance in terms of life-to-rupture, temperature capability or allowable stress, and better low-cycle fatigue performance, which should increase chamber lifetime.

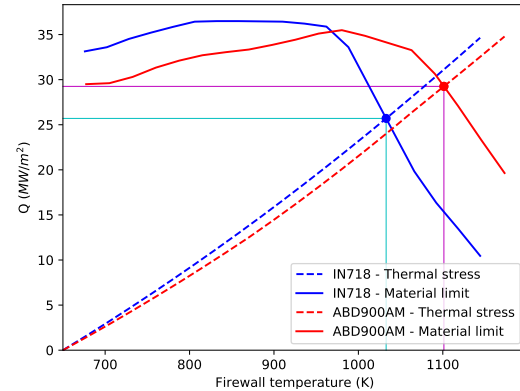


Figure 2: Maximum theoretical heat flux for reaching the yield stress of IN718 and ABD<sup>®</sup>-900AM based on the firewall temperature and assumed coolant side temperature of 650K, for firewall thickness of 0.3mm.

#### 4. ABD<sup>®</sup>-900AM TEST PIECES

Small test pieces were printed on a RENAM 500Q to verify that the required combustion chamber geometry would be adequately formed. Fig. 3 shows a few of these, that were printed for a combustion chamber with conservative firewall thickness of 1.0mm. Samples were printed whilst tuning laser parameters for achieving good part density. Although some minor porosity was seen no HIP process was applied.

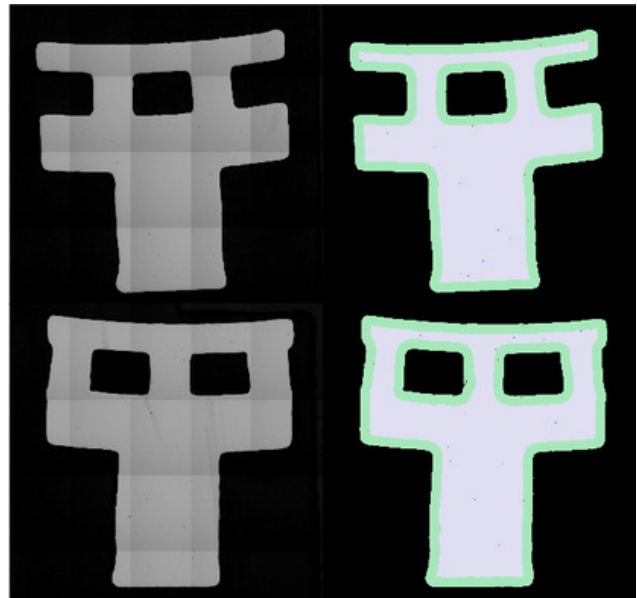


Figure 3: Test pieces as-printed in ABD<sup>®</sup>-900AM to examine part density (no HIP treatment). Credit Renishaw plc.



Figure 4: First combustion chamber test pieces (v1.0) with ABD<sup>®</sup>-900AM on the left and IN718 on the right.

## 5. COMBUSTION CHAMBER DEMONSTRATOR

### 5.1. ABD<sup>®</sup>-900AM and IN718 chamber v1.0

A small combustion chamber demonstrator was designed to perform initial hot firings and test the manufacturing process. The chamber was designed to be used with an existing liquid bi-propellant feed system using Isopropyl alcohol (IPA) and Nitrous Oxide propellants (N<sub>2</sub>O). This was previously used with a throttleable pintle injector for evaluating combustion chambers additively manufactured in CuCrZr [14]. High pressure water cooling is used in order to separate the cooling and combustion processes and therefore make it easier to throttle the heat flux.

The design has a 70mm combustion chamber and 25mm throat, in order to re-use the existing injector head [14]. It has helical coolant channels in the cylindrical section of the combustion chamber in order to evaluate the surface roughness of printed channels with long sections of upskin and downskin. Helical channels are commonly used in small combustion chambers in order to maintain sufficient flow velocity in the chamber section for cooling without requiring small channels. Coolant channels in the nozzle contraction, throat and expansion were kept axial for simplicity. There are integral coolant inlet (nozzle end) and outlet manifolds (injector end), and a separate film cooling manifold for film cooling experiments.

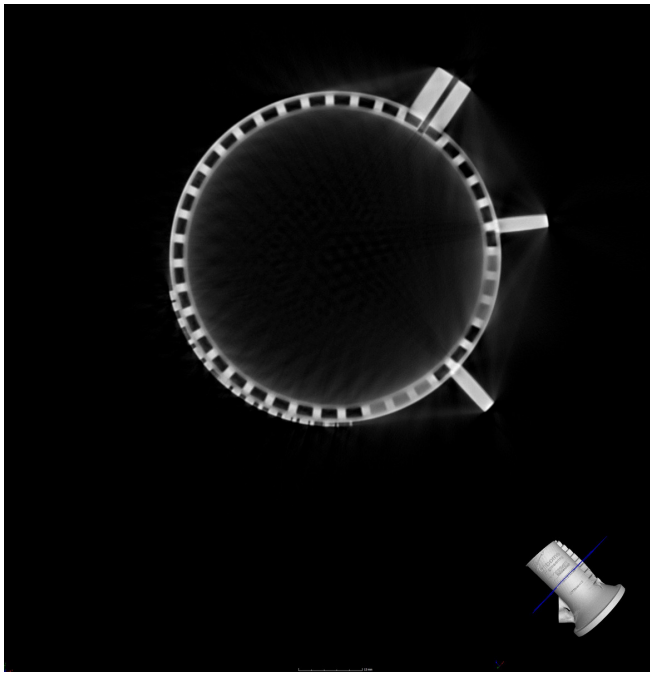
Three rows of instrumentation bosses were included, two rows into the coolant channels and one row for measuring the firewall temperature down the middle of the fins. Fig. 4 shows the v1.0 combustion chambers, which were printed in both ABD<sup>®</sup>-900AM

and IN718. The helical twist of the channels in the cylindrical section can easily be seen from the tapings, which each follow a particular coolant channel.

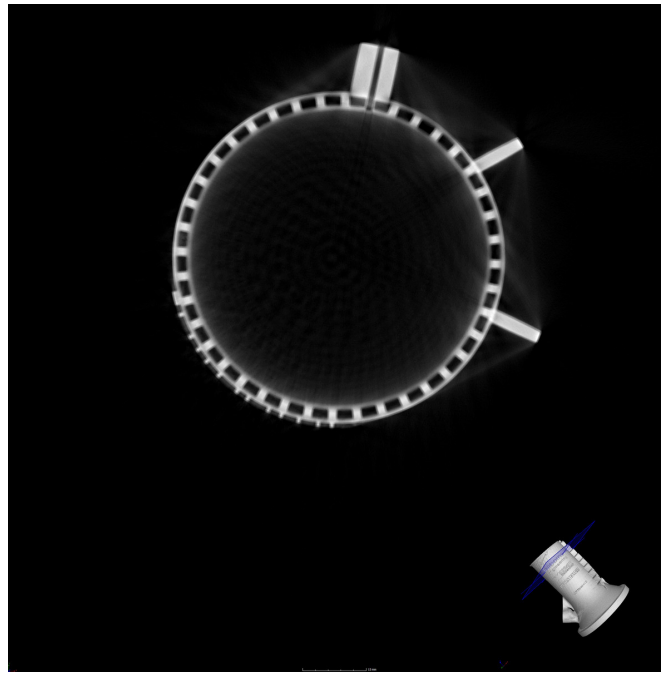
The firewall in the v1.0 chamber was 1.0mm thick, and walls between channels were thick due to manufacturer hesitancy with printing thin walls in the first iteration. The maximum permissible heat flux is inversely proportional to wall thickness (eq. 3), and for nickel alloy chambers a 1.0mm firewall would be impractical for high performance engines and only suitable for low chamber pressures. A lower wall thickness was used for subsequent chambers and firings.

As expected, the surface finish of the ABD<sup>®</sup>-900AM chamber was noticeably much better than that of the IN718 chamber. As such, the ABD<sup>®</sup>-900AM chamber would have the advantages of lower coolant pressure drop, and if left unpolished a lower hot-gas heat flux. Both materials were similar to post-machine.

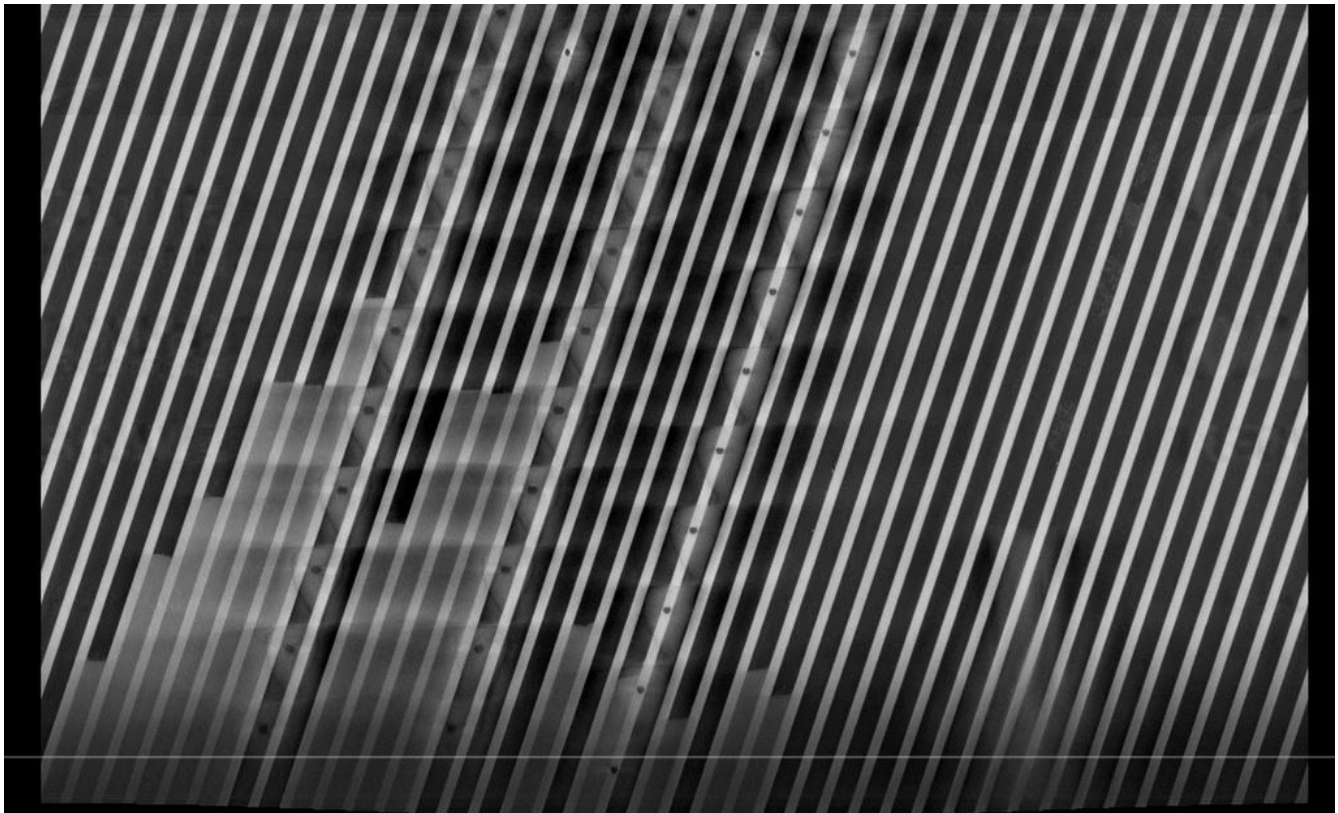
The v1.0 chambers were not used for hot firing because they were found to have powder blockages after the heat treatment step, which was confirmed by CT scanning (Fig. 5). It is not clear whether the failure to completely depowder the chambers was down to lack of attention during de-powdering procedures, or simply that the geometry only allowed the channels to be blown through in parallel - i.e. it was not possible to blow through one channel alone and ensure that it was depowdered. Blowing through in parallel also reduces the efficiency of the process, in that when several channels are clear, the air will preferentially flow through these and ignore the still blocked channels. Increased NDT steps and de-powdering aids were included in the next design iteration.



(a) Blocked coolant channels (lower right quadrant)



(b) Unblocked coolant channels



(c) Summary of CT scans in 'unrolled' form, which clearly shows the powder blockages, channels and instrumentation tappings.

Figure 5: Example CT Scan results for the ABD<sup>®</sup>-900AM v1.0 chamber with (a) blocked and (b) unblocked channels, and (c) an 'unrolled' CT scan showing the powder blockages.



(a) On build-plate with powder access holes

(b) Post-machined

Figure 6: ABD®-900AM v1.1 chamber, showing (a) as-built and (b) post-machined geometry. The ring of small powder-access upstands on the build plate allows powder to be blown/vacuumed from each individual channel, to ensure powder removal prior to heat treatment. These tubes are wire-eroded off before post-machining.

## 5.2. ABD®-900AM chamber v1.1

A v1.1 combustion chamber was redesigned and printed in ABD®-900AM taking into account the issues encountered with the v1.0 design. Most of the geometry was identical with a few notable differences. The v1.1 chamber was printed with a much thinner firewall of ~0.3mm (instead of 1.0mm for v1.0) and thinner walls between coolant channels. A thinner outer closeout to the channels was also used to make the chamber closer to a flightweight configuration - albeit still with a heavy outlet manifold and injector interface flange for ground testing to make it interchangeable with the current water coolant system.

To assist de-powdering, each coolant channel was blocked where it entered the outlet manifold with a small cap, that could be easily drilled out during post machining. Small tunnels were then created to each

channel through the flange face to small powder access upstands. Fig. 6a shows the chamber on the build plate with the ring of powder access upstands. This allowed each channel to be blown through individually, and the resultant outflow from the coolant inlet fitting noted to ensure complete depowdering. The powder access upstands and tunnels could then be wired off before post-machining. Some custom blowing tools were created to assist in this process. A stricter de-powdering process was followed, and the chamber was checked before proceeding to heat treatment. Once heat treated and the bosses post-machined, the chamber was subjected to a water flow test before the caps on each channel were drilled out to join the channels to the coolant outlet manifold. This allowed a qualitative check that all channels were free of powder or swarf.

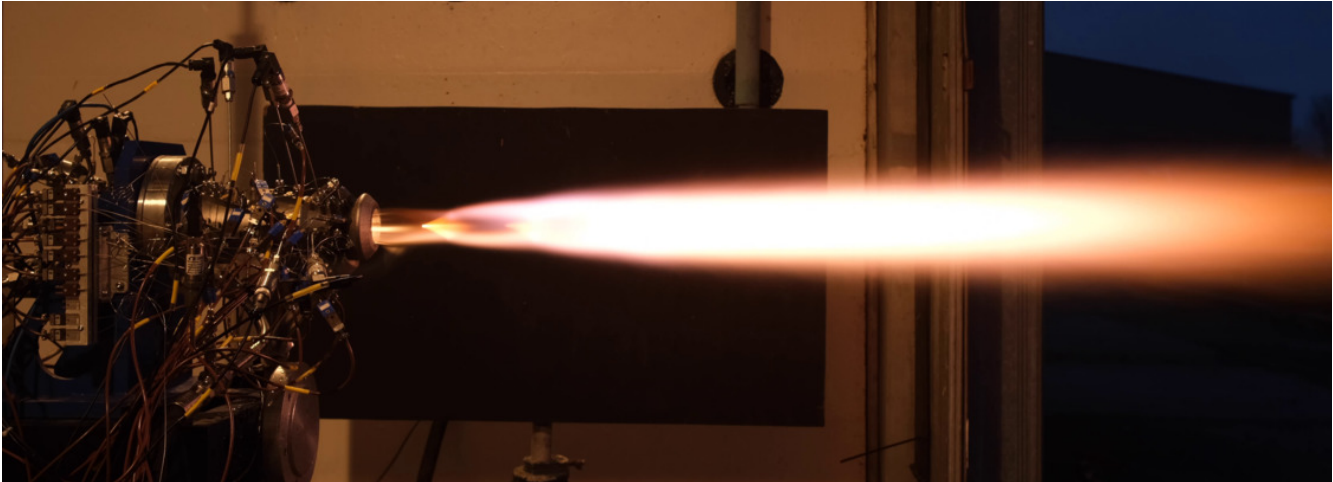


Figure 7: Firing of the first additively manufactured ABD<sup>®</sup>-900AM combustion chamber (v1.1) using liquid bipropellants.

Before hot-firing the chamber was hydraulically tested to check the integrity of the firewall. Unfortunately the v1.1 chamber failed this test because the firewall had pinhole leaks. Subsequent analysis suggested that the laser parameters could have been improved for the thin-wall areas.

It was decided to hot-fire the chamber anyway to demonstrate the end-to-end design. The hot-firing was undertaken in the J1 firing bay at the AEL test site in Westcott (UK). Instrumentation such as pressure sensors and thermocouples were used to monitor propellant injector supplies, and to record the pressure drop and temperatures in the coolant channels and the temperature of the coolant side of the firewall. An exit choke provided backpressure to the water coolant supply to raise the boiling point and increase the maximum heat flux permissible. By using a pressure sensor upstream of the choke the coolant massflow could be calculated using a catch-and-weigh calibration procedure. Data was recorded using AEL's in house data acquisition system at 10kHz, simultaneously across all sensors.

Fig. 7 shows the demonstration firing at a chamber pressure of 20bar (predicted maximum heat flux  $\sim 14\text{MW/m}^2$ ) with no visible damage to the combustion chamber. The coolant pressure drop was similar to predictions suggesting a reasonable surface finish on the inside of the channels. Coolant side firewall surface temperatures measurements were close to predicted but slightly lower, likely due to film cooling from the pinhole leaks, which will have reduced the maximum firewall temperature and also caused the exhaust plume to appear blurry, as in Fig. 7.

### 5.3. ABD<sup>®</sup>-900AM chamber v1.2

A v1.2 combustion chamber was printed to solve the issues found with the v1.1 chamber. Most of the geometry was identical, but there were minor geometry changes around small holes, a more qualified set of laser parameters was used in the thin wall areas, and the web supporting the inlet boss was thickened. The instrumentation bosses were printed with a thin blanking cap (removed by subsequent machining), which in conjunction with a threaded inlet boss and a rubber seal over the powder-access upstands, allowed the chamber to be pressure tested whilst still on the baseplate. This allowed verification of firewall integrity (no pinholes) without requiring further operations such as machining or heat treatment.

The v1.2 chamber passed the pressure test and was subsequently post-machined and heat treated. A flow test verified that no coolant channels were blocked and that there was not significant flow variation between channels. Fig. 8 shows the v1.2 chamber during initial hot-firing testing. Both Fig. 7 and 8 are taken at the same operating point (chamber pressure 20bar), but there is a noticeably cleaner exhaust plume for the v1.2 chamber which does not have pinhole leaks. Testing of the v1.2 chamber is ongoing.

Further work to evaluate the effectiveness of the ABD<sup>®</sup>-900AM alloy for combustion chamber manufacture requires higher heat flux firings, ideally with increasing heat load until destruction, with performance compared against that for an identical IN718 chamber. This would be best undertaken in parallel with further material property tests on printed samples.

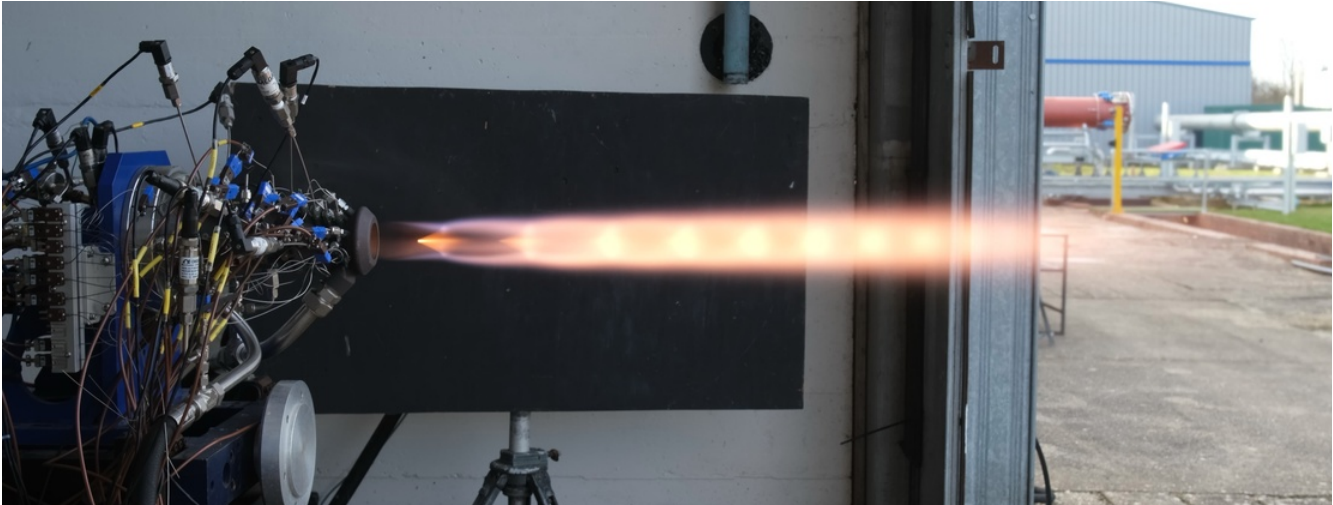


Figure 8: Firing of the additively manufactured ABD<sup>®</sup>-900AM combustion chamber (v1.2).

## 6. CONCLUSIONS

The new ABD<sup>®</sup> series of alloys have been designed specifically for additive processes, with the ABD<sup>®</sup>-900AM alloy able to maintain strength up to 900°C, demonstrating an increase in temperature capability over IN718 of ~100°C. A simple firewall thermal stress analysis suggests that this could enable heat fluxes of order ~14% higher than those for IN718, leading to a ~18% higher chamber pressure and therefore higher specific impulse. Improvements in surface roughness are also expected and were seen in printed components. These benefits are possible by only changing the powder and keeping laser parameters the same, which make switching to ABD<sup>®</sup>-900AM relatively easy without fully requalifying processes.

Demonstrator combustion chambers were designed and built in ABD<sup>®</sup>-900AM resulting in the first hot firing of rocket engine components made from ABD<sup>®</sup> alloys. The initial firings were positive, with no visible damage to the combustion chamber. Further experimental work is required to confirm the predicted increase in maximum heat flux over that of IN718, and further theoretical work and materials tests are required to evaluate the predicted chamber lifetimes.

## 7. ACKNOWLEDGEMENTS

The authors would like to thank the team at Alloyed (formerly OxMet Technologies and Betatype) and the Renishaw solution centre for their expertise and partnership in this programme.

## REFERENCES

- [1] Roback, R. et al. (1981). Deposit formation in hydrocarbon rocket fuels, *NASA CR-165405*.
- [2] Soller, S. et al. (2017). Design and Testing of Liquid Propellant Injectors for Additive Manufacturing, *7th European Conference for Aerospace Sciences (EUCASS)*.
- [3] Gradl, P. et al. (2018). Additive Manufacturing of Liquid Rocket Engine Combustion Devices: A Summary of Process Developments and Hot-Fire Testing Results, *54th AIAA/SAE/ASEE Joint Propulsion Conference*.
- [4] Müller, I. et al. (2018). 3D Printed coaxial injector for a LOX/Kerosene rocket engine, *Space Propulsion Conference*.
- [5] Gradl, P. (2017). Additive Manufacturing Overview: Propulsion Applications, Design for and Lessons Learned
- [6] Gradl, P. et al. (2019). Bimetallic channel wall nozzle development and hot-fire testing using additively manufactured laser wire direct closeout technology, *AIAA Propulsion and Energy Forum and Exposition*.
- [7] Gradl, P. et al. (2019). Additive manufacturing development and hot-fire testing of liquid rocket channel wall nozzles using blown powder directed energy deposition inconel 625 and jbk-75 alloys, *AIAA Propulsion and Energy Forum and Exposition*.
- [8] Reed, R. et al. (2016). Alloys-by-design: Towards

optimization of compositions of nickel-based superalloys. *Proceedings of the 13th International Symposium of Superalloys*.

- [9] Reed, R. (2015). Method for designing alloys. *US10872682B2*.
- [10] Roark, R. and Young, W. (1975), Formulas for stress and strain, Fifth Edition, McGraw Hill.
- [11] Ziebland, H. and Parkinson, B. (1971). Heat transfer in rocket engines, *AGARD-AG-148-71*.
- [12] Giovanetti, A. et al. (1984). Deposition formation and heat transfer in hydrocarbon rocket engines, *AIAA 22nd Aerospace Sciences Meeting*.
- [13] Special Metals (2007). Inconel alloy (IN718) datasheet, *Special Metals Corporation*.
- [14] Waugh, I. et al (2021). Additive manufacture of rocket engine combustion chambers from Cu-CrZr (C-18150) using the DMLS process, *Space Propulsion 2020+1*.